Nonlinear Dynamics (2005) 42: 383–394

Estimation of Chaotic and Regular (Stick–Slip and Slip–Slip) Oscillations Exhibited by Coupled Oscillators with Dry Friction

J. AWREJCEWICZ[1], L. DZYUBAK[2], and C. GREBOGI[3,*]

[1]*Division of Automatics and Biomechanics (K-16), Technical University of Lodz, 1/15 Stefanowskiego Street, 90-924 Lodz, Poland;* [2]*Department of Applied Mathematics, Kharkov Polytechnic University, 21 Frunze Street, 61002 Kharkov, Ukraine;* [3]*Instituto de Fisica, Universidade de São Paulo, Caixa Postal 66318, 05315-970 São Paulo, Brazil;*
[*]*Author for correspondence (e-mail: grebogi@if.usp.br; fax: +55 11-3091-6749)*

(Received: 15 November 2004; accepted: 27 April 2004)

Abstract. In this paper, we present a novel approach to quantify regular or chaotic dynamics of either smooth or non-smooth dynamical systems. The introduced method is applied to trace regular and chaotic stick–slip and slip–slip dynamics. Stick–slip and slip–slip periodic and chaotic trajectories are analyzed (for the investigated parameters, a stick–slip dynamics dominates). Advantages of the proposed numerical technique are given.

Key words: coupled oscillators, chaotic dynamics, stick–slip, slip–slip motion

1. Introduction

Simple dynamical oscillators exhibiting chaotic behavior are still a topic of investigation, but a richer dynamics is exhibited by coupled oscillator systems and it has inspired a great deal of research [1–3]. Various real systems in mechanics [4–6], electro-mechanics [7–9], and life sciences [2, 10] are modeled by coupled oscillators. Among them a special class of important (both from the point of view of theory and application) systems are those excited by dry friction [4–6, 11].

In this work, our attention is focused on the analysis of self-excited 2-degrees-of-freedom coupled system with dry friction. First, an approach to quantify chaos is addressed, and then the domains of stick–slip and slip–slip oscillation are investigated.

The descriptions of various prognostic and diagnostic criteria of chaos occurring in nonlinear dynamical systems can be found in numerous introductory books on chaos. To such known approaches, it is possible to mention Melnikov's method, period doubling criteria, "Smale horseshoe", spectrum analysis, the method of cell-to-cell mapping for nonlinear dynamical systems [14–16] and the most often exploited Lyapunov exponents' computations, etc.

No belittling merits of the analytical approaches, it should be mentioned that for some comparatively simple equations, the theoretical criteria of appearance of chaos have not been found yet. Even though the Melnikov's method for systems in R^n has been presented [17], only periodically forced dynamical systems with a small parameter are considered. In addition, for such systems, it is necessary to know the homoclinic orbit explicitly. But for most of nonlinear dynamical systems, finding an analytical expression for the homoclinic orbit is virtually impossible. The upshot, the algorithms for the realization of Melnikov's approach for computing the bifurcation conditions are based on numerical simulations. Furthermore, the theoretical thresholds, which correspond to the homoclinic trajectory criterion, are known to be underestimated and do not reflect the complex structure of chaotic regions (and presence of

periodic "windows", chaotic "islets", "streaks" etc.). Also it is known that during a treatment of bifurcations, the validity of analytical methods is often only local. Both analytical and numerical approaches must be used together to confirm the chaotic character of the motion in the investigated regions.

The question of universal multipurpose criteria for analysis of nonlinear dynamical systems is still open. During implementation of existent approaches various difficulties and problems arise. Later, we briefly describe two effective approaches for nonlinear dynamical systems analysis and give comparative valuation and advantages of the approach presented in this paper.

Hsu's method of cell-to-cell mapping for nonlinear dynamical systems [14–16] is an interesting non-ordinary approach. The procedure of the algorithm is devised by taking advantages of certain properties of Markov chains as tools for global analysis of the mapping systems. The generalized cell-mapping theory is theoretic base for computer algorithms for the systems analysis involving a very large number of cells. But it is computationally intensive. Let us illustrate it. Let a cell $\mathbf{Z}(n)$ be mapped by the mapping $\mathbf{G}$. According to the generalized theory of cell-to-cell mapping, the mapping of a cell $\mathbf{Z}(n)$ may have several possible image cells, each image cell having a definite fraction of the total number of possibilities. In another words, if the system is at cell $\mathbf{Z}(n)$ when $t = n$, the state at the next step $t = n + 1$ can be at $\mathbf{Z}^{(1)}(n + 1)$ with probability $p^{(1)}$, at $\mathbf{Z}^{(2)}(n + 1)$ with probability $p^{(2)}$, and so forth. The state of the system is described by the probabilities according to which state the system may be found. In that way, for each fixed set of control parameters, a "sink cell" is introduced and is labeled number 0, and then other cells are labeled 1, 2, ... , N. The cells are classified as *persistent* or *transient* cells. The persistent cells are decomposed into *irreducible persistent groups*. The period of each persistent group and the long-term *limiting probability distribution* among the cells within each group (for the *acyclic groups* and for the *periodic groups*) are determined. Then the evolution from all the transient cells by computing the *absorption probability* α_{ij} of a transient cell j into a persistent cell i, the *groups absorption probability* $\alpha(\mathbf{B}_g, j)$ of cell j into a persistent group $\mathbf{B}_g$, and the *expected absorption time* ν_j of cell j into persistent groups are evaluated. The probabilities of mappings among cells are defined using different schemes as, for instance linear (or higher-order) interpolation methods. Method of analyzing generalized mappings implies also in computer intensive operations with matrices. The most time-consuming part of the algorithm is the evaluation of the matrix that characterizes the expected absorption time. This matrix results from the inversion of a high order very sparse matrix. To find the inverse of such a matrix is a time consuming task. Therefore, special sparse matrix techniques are used. There are also other technical problems.

The Wolf's algorithm for determining the Lyapunov exponents can also be realized by computer simulation. Even in presence of fast computers, recent scientific books [18] have pointed out problems which appear using standard procedures of Lyapunov exponent calculations in practice. According to Wolf's algorithm, the calculation of the Lyapunov exponent λ as the measure of the trajectory divergence begins with the choice of a basic trajectory $\mathbf{x}^*(t, \mathbf{x}^{(0)})$. At each time step t_k the dynamical system is integrated along with any neighboring point $\mathbf{x}^*(t_k)+\eta$ acting as the initial condition. To find the exponent λ, the governing equations and the corresponding variational equations $\dot{\eta} = \mathbf{A} \cdot \eta$, in which $\mathbf{A}$ is matrix of partial derivatives $\nabla f(\mathbf{x}^*(t_k))$, are solved N times (where N is the number of the time steps). The averaging over long times results in a reliable value of λ. The analogous calculation needs to be executed for all nodal points of the sampled space under investigation. This procedure is very computationally intensive especially for non-smooth systems. The method can often work for low-dimensional systems, but in practice, it fails for chaotic systems of high-dimensionality. To carry out our approach, it is enough to solve the equations governing the dynamical system only two times for each selected trajectory. For our specific problem, the characteristic vibration amplitudes A_i is calculated simultaneously with the integration of the trajectory. So, for each selected trajectory it does not have to find the matrix of partial

derivatives A, and the governing differential set is solved 2 times instead $2N$, not having to average over a long times the distances between the trajectories.

Note that calculations of Lyapunov exponents may results also in other problems [18]. On the one hand, the individual terms of the cumulative product matrix grow exponentially, and, on the other hand, the eigenvectors all tend to align themselves in the direction of the maximum growth and hence do not accurately span the space. To avoid these problems, the Gram–Schmidt orthonormalization may be used additionally, but it increases the time consumed and it also complicates the algorithm.

The chaotic trajectories, which are quantified using our approach, correspond to "positive" Lyapunov exponents. Even in the case of calculating the largest Lyapunov exponents without having to calculate the matrix of partial derivatives, the present approach still remains simpler and less time-consuming (especially for discontinuous systems and for systems of higher dimensionality). Transient chaos (in which the motion is apparently chaotic for a long time before eventually settling down to a nonchaotic attractor) often occurs near a global bifurcation, signaling the onset of chaos. The resulting regions of chaotic motion include cases of transient and alternating chaos. Even with this restriction for the various investigated smooth and non-smooth systems, our approach reflects extremely well the complex structure of chaotic regions (presence of periodic "windows", chaotic "islets", "streaks" etc.).

2. The Model

Consider two masses m_1 and m_2 (as shown in Figure 1) which are riding on a driving belt. The belt is moving at a constant velocity v_0. The mass m_1 is attached to a wall by a spring k_1. Masses m_1 and m_2 are coupled by a spring k_2. A friction force T_i acts between the mass m_i and the belt which is dependent on the relative velocity w_i $(i = 1, 2)$ between both. These 2-degree-of-freedom autonomous oscillators are governed by the following second-order set of coupled differential equations

$$\begin{cases} m_1\ddot{x}_1 = -k_1x_1 - k_2x_1 + k_2x_2 + T_1(w_1) \\ m_2\ddot{x}_2 = -k_2x_2 + k_2x_1 + T_2(w_2), \end{cases} \tag{1}$$

where

$$w_i = v_0 - \dot{x}_i \quad (i = 1, 2).$$

For the $T_i(w_i)$, we consider the following friction model (see Figure 2):

$$T_i(w_i) = T_{0i}\ \mathrm{sign}(w_i) - \alpha_i(T_{0i})w_i + \beta_i(T_{0i})w_i^3,$$
$$\alpha_i = \frac{3}{4}\frac{T_{0i}}{v_i^*} \quad \beta_i = \frac{T_{0i}}{4(v_i^*)^3} \quad (i = 1, 2).$$

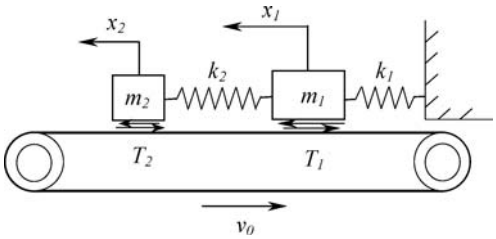

Figure 1. Autonomous coupled oscillators with friction.

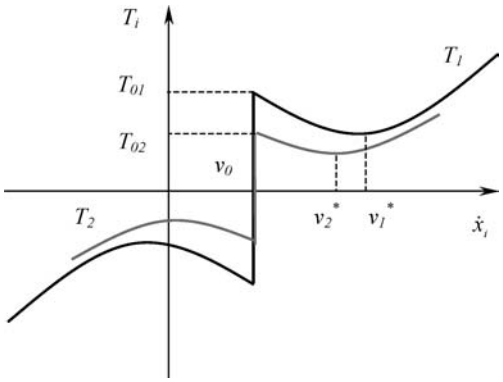

Figure 2. Friction model.

Here the maximum static friction force is denoted by T_{0i}, and v_i^* is the velocity corresponding to the maximum value of $T_i(w_i)$ $(i = 1, 2)$ (Figure 2).

3. Our Approach and the Analysis of the Wandering Trajectories

The chaotic behavior of nonlinear dynamical systems can have different physical manifestations. For example, an external periodic excitation applied to a multi-well potential system may cause a chaotic response. In this case, the unpredictable switches between the potential wells characterize the chaotic behavior. Other factors may result in unpredictable changes of the vibration amplitude of the trajectories. This manifested unpredictability of the chaotic trajectories is affirmed by stating that those systems exhibit sensitive dependence on the initial conditions. By analyzing the trajectories of those systems, it is possible to find the chaotic vibration regions in control parameter space.

Let a dynamical system be expressed by the following set of ordinary differential equations

$$\dot{\mathbf{x}} = f(t, \mathbf{x}), \tag{2}$$

where $\mathbf{x} \in R^n$ is the state vector, $f(t, \mathbf{x})$ is defined in $R \times R^n$ and is the time derivative of the state vector. It is assumed, that $f(t, \mathbf{x})$ is smooth enough to guarantee existence and uniqueness of a solution of the set (2). The right-hand side can be discontinuous, while the solution of the set of differential equations (2) remains continuous. For instance, in cases of discontinuous vector fields of the "transversal intersection" and "attracting sliding mode" types a solution of the set (2) exists and is unique. In that way, the continuous dependence property on the initial conditions $\mathbf{x}^{(0)} = \mathbf{x}(t_0)$ of the solution of the set (2) is used: *for all initial conditions* $\mathbf{x}^{(0)}$, *and* $\tilde{\mathbf{x}}^{(0)}$, *both in* R^n *and at* $t = 0$, *for every number* $T > 0$, *no matter how large, and for every pre-assigned arbitrary small* $\varepsilon > 0$ *it is possible to find a positive number* $\delta > 0$ *such that if the distance* ρ *between* $\mathbf{x}^{(0)}$ *and* $\tilde{\mathbf{x}}^{(0)}$ *is* $\rho(\mathbf{x}^{(0)}, \tilde{\mathbf{x}}^{(0)}) < \delta$, *and for* $t \leq T$, *takes place the inequality*

$$\rho(\mathbf{x}(t), \tilde{\mathbf{x}}(t)) < \varepsilon.$$

In another words, if the initial points are chosen close enough, then during the pre-assigned arbitrary large time interval $t \leq T$ the distance between simultaneous positions of moving points are less given then a positive number ε.

Since we are interested in identifying chaotic and regular dynamics, we assume that all trajectories remain in the closed bounded domain of a phase space, i.e.

$\exists C_i \in R : \max_t |x_i(t)| \leq C_i \quad (i = 1, 2 \ldots n).$

If a trajectory escapes to infinity, it may be diagnosed easily.

To analyze trajectories of the set (2), we introduce the characteristic vibration amplitudes A_i of the components of the motion $x_i(t)$:

$$A_i = \frac{1}{2}\left| \max_{t_1 \leq t \leq T} x_i(t) - \min_{t_1 \leq t \leq T} x_i(T) \right| \quad (i = 1, 2 \ldots n).$$

$[t_0, T]$ is the time interval, in which the motion is considered, $[t_0, t_1]$ is the time interval in which all transient processes are damped.

Though a metric ρ on R^n can be assigned in various ways, we find it convenient to consider an n-dimensional parallelepiped defined through the embedding theorem, which states as follows:

if $S_\varepsilon(\mathbf{x}) = \{\tilde{\mathbf{x}} \in R^n : \rho(\mathbf{x}, \tilde{\mathbf{x}}) < \varepsilon\}$ *is the hyper-sphere with center in the point* $\mathbf{x}$ *and with radius* ε *and* $P_{\varepsilon_1,\varepsilon_2,\ldots,\varepsilon_n}(\mathbf{x}) = \{\tilde{\mathbf{x}} \in R^n : |x_i - \tilde{x}_i| < \varepsilon_i\}$ *is the n-dimensional parallelepiped, then for any* $\varepsilon > 0$ *there is parallelepiped* $P_{\varepsilon_1,\varepsilon_2,\ldots,\varepsilon_n}(\mathbf{x})$ *such that* $P_{\varepsilon_1,\varepsilon_2,\ldots,\varepsilon_n}(\mathbf{x}) \subset S_\varepsilon(\mathbf{x})$. *And conversely, for any parallelepiped* $P_{\varepsilon_1,\varepsilon_2,\ldots,\varepsilon_n}(\mathbf{x})$ *it is possible to indicate* $\varepsilon > 0$ *such that* $S_\varepsilon(\mathbf{x}) \subset P_{\varepsilon_1,\varepsilon_2,\ldots,\varepsilon_n}(\mathbf{x})$.

Let us choose in the parallelepiped $P_{\delta_1,\delta_2,\ldots,\delta_n}(\mathbf{x}^{(0)})$ two neighboring initial points $\mathbf{x}^{(0)}$ and $\tilde{\mathbf{x}}^{(0)}$, such that $|x_i^{(0)} - \tilde{x}_i^{(0)}| < \delta_i$, where δ_i is small in comparison with A_i $(i = 1, 2 \ldots n)$. For the case of regular motion, it is expected that the ε_i in the inequality $|x_i(t) - \tilde{x}_i(t)| < \varepsilon_i$ is also small in comparison with A_i $(i = 1, 2 \ldots n)$. The wandering orbits attempt to fill some bounded domain of the phase space. The trajectories that are close at the instant t_0 diverge exponentially on the average afterwards. Hence, the absolute values of differences $|x_i(t) - \tilde{x}_i(t)|$ for some instant t_1 can take any values in the interval $[0, 2A_i]$. If the differences $|x_i(t) - \tilde{x}_i(t)|$ are equal to zero at some instants $\{t_k^*\}$, $(t_k^* \in [t_1, T])$ then the trajectories $\mathbf{x}(t)$ and $\tilde{\mathbf{x}}(t)$ are coincident at those instants. Obviously, $2A_i$ are the maximum values of these differences. And it is quite admissible value for some time instants. Let us introduce an auxiliary parameter α, $0 < \alpha < 1$. The αA_i are the divergence measures of the observable trajectories in the directions of the generalized coordinates x_i $(i = 1, 2, \ldots n)$. By analyzing Equation (2) and its equilibrium states, it is easy to choose an α parameter, $0 < \alpha < 1$, such that from the truth of the statement

$$\exists t^* \in [t_1, T] : |x_i(t^*) - \tilde{x}_i(t^*)| > \alpha A_i \quad (i = 1, 2, \ldots, n), \tag{3}$$

it follows that there is a time interval or set of time intervals, for which the trajectories $\mathbf{x}(t)$ and $\tilde{\mathbf{x}}(t)$ move around various equilibrium states. These trajectories are sensitive to changing the initial conditions. Thus, these trajectories are wandering. Indeed, as it has already been mentioned, all trajectories are in the closed bounded domain of the space R^n. With the aid of the parameter α, we choose the divergence measures of the trajectories αA_i, which are *inadmissible* for the case of 'regularity' of the motion. Note that this choice is non-unique and the α parameter can take various values on the interval (0, 1). But it is clear, that if α is near 0 and $|x_i(t) - \tilde{x}_i(t)| < \alpha A_i$ when $t \in [t_0, T]$, then the trajectories do not diverge and are hence regular. There are values of the α parameter, which a priori corresponds to the inadmissible divergence measures αA_i $(i = 1, 2, \ldots n)$ of the trajectories in the sense of 'regularity'. For example, $\alpha \in \{\frac{1}{3}, \frac{1}{2}, \frac{2}{3}, \frac{3}{4}\}$ but other choices are possible. If the representative points of the observable trajectories move chaotically, then for another choice α from the set of a priori 'appropriate' α, the divergence of the trajectories will be recorded at another time t^*. As numerical experiments show, the obtained domains of chaotic behavior with various a priori 'appropriate' values of the α parameter are practically congruent. Therefore, in this work, pictures for different values of α are not presented.

A similar non-unique choice of parameters occurs when applying some other criterium for the chaotic oscillations. For instance, one can apply the procedure for calculating the Lyapunov exponents $d(t) = d_0 2^{\lambda t}$. Here λ is Lyapunov exponent, d_0 is the initial distance measure between the starting points, $d_{(t)}$ is the distance between trajectories at instant t. The base 2 is chosen for convenience. In all other respects, the parameter $\alpha > 1$ in the relation $d(t) = d_0 \alpha^{\lambda t}$ is arbitrary. That is, the α parameter can take values, for example, $\alpha \in \{2, 3, 4, 5\}$ but other choices are possible. In general, the specificity of the numerical approach is like that, all parameters have to be concrete and most of them can be non-unique.

By varying the parameters of the system, and using condition (3), it is possible to find domains of chaotic motions (including transient and alternating chaos) and domains of regular motions. This approach has been realized on well-known systems – the non-autonomous Duffing equation and Lorenz system [12]. It has achieved remarkable results and very good agreement with other investigations.

4. A Stick–Slip and Slip–Slip Motions

Let us find the stick–slip and slip–slip domains of the chaotic or regular motion. If the solution $\mathbf{x}(t)$ of the set (1) is known, it is easy to obtain the set of time intervals $\{\Delta t_{\mathrm{st}\,i}\}$ for which

$$\dot{x}_i = v_0 \quad (i = 1, 2). \tag{4}$$

It corresponds to the presence of "stick" in the vibrations of ith oscillator. The maximum time interval $\max \Delta t_{\mathrm{st}\,i}$ from the set $\{\Delta t_{\mathrm{st}\,i}\}$ can be considered as a characteristic of a given motion.

If the investigated space of parameters has as one of its coordinates the velocity of the belt v_0, the dynamics of the process increases with magnification of v_0. And then even very small $\max \Delta t_{\mathrm{st}\,i}$ does point out the presence of the "stick" in the vibrations. In this case, under appropriate choice of the constant $0 < \delta < 1$, and by checking the control condition

$$v_0 \ \max \Delta t_{\mathrm{st}\,i} > \delta A_i \quad (i = 1, 2), \tag{5}$$

it allows to trace the presence of "stick" motion, which could be lost in the analysis using $\max \Delta t_{\mathrm{st}\,i}$.

5. Results and Discussion

The conditions (3) for the system (1) can be presented in the following form

$$\begin{array}{c} \exists t^* \in [t_1, T]: \\ \{(|x_1(t^*) - \tilde{x}_1(t^*)| > \alpha A_1) \vee \quad (|x_2(t^*) - \tilde{x}_2(t^*)| > \alpha A_2)\} \\ \Downarrow \qquad\qquad\qquad\qquad \Downarrow \\ \text{chaos of the first oscillator} \quad \text{chaos of the second oscillator} \end{array} \tag{6}$$

Fulfillment of the condition $(|x_1(t^*) - \tilde{x}_1(t^*)| > \alpha A_1) \wedge (|x_2(t^*) - \tilde{x}_2(t^*)| > \alpha A_2)$ signifies a presence of hyper-chaotic behavior of the system.

Using the conditions (4)–(6), the space of parameters (v_0, T_{01}, T_{02}) for the system (1) is investigated after a coordinate sampling with a grid width $\Delta v_0 = 0.1$, $\Delta T_{01} = 1$, $\Delta T_{02} = 1$. The domains in which the chaotic behavior of the first and second oscillators occurs are found. The domains of stick–slip and slip–slip motion are also found. All numerical calculations are done for the following fixed values, characterizing the system (1): $m_1 = 4$, $m_2 = 3$, $k_1 = 11.77$, $k_2 = 7.85$, $v_1^* = 4$, $v_2^* = 3$. The following

initial conditions are taken: $x_1(0) = 0.01$, $\dot{x}_1(0) = 0.5$, $x_2(0) = 0.01$, $\dot{x}_2(0) = 0.5$. The time history of the trajectories of motion is 120 units. During simulations, a half of this time corresponds to the time interval $[t_0, t_1]$, in which the transitional processes are damped. Initial conditions of the closed trajectories are distinguished by 0.5% with ratio of characteristic vibration amplitudes A_i $(i = 1, 2)$, and α parameter to be equal to 1/3.

Figure 3 in the section $T_{02} = 19.62$ of the parameter space (v_0, T_{01}, T_{02}) represents the domains where chaotic vibrations of the first (a) and of the second (b) oscillators are possible. It is interesting, that these regions are almost congruent. That is, one does not observe the situation when only one of the oscillators moves chaotically. It is also remarkable, that the presence of the chaotic "islets" in the domains of periodic movement is also characteristic of many experiments in chaotic dynamics. In the cross-section $T_{01} = 29.43$ (see Figure 4) the chaotic vibrations domains of first (a) and second (b) oscillators are also practically congruent.

In Figures 5 and 6, the domains of stick–slip oscillations are exhibited, corresponding to various "adhesion" time Δt_{st} of the oscillators to the belt (when $5 < \max \Delta t_{\text{st}\,i}$, $2 < \max \Delta t_{\text{st}\,i} < 5$, $0.5 < \max$

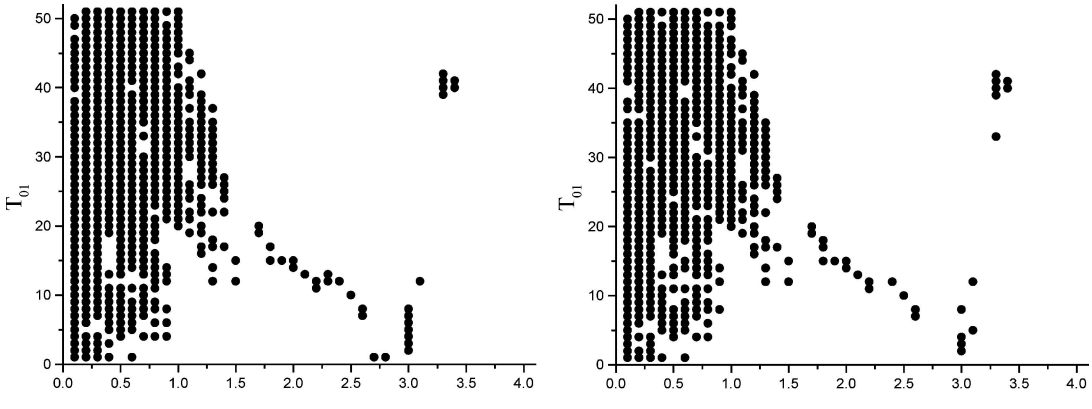

Figure 3. Domains of chaotic vibrations of the first (a) and of the second (b) oscillators in the (v_0, T_{01}) plane at $T_{02} = 19.62$.

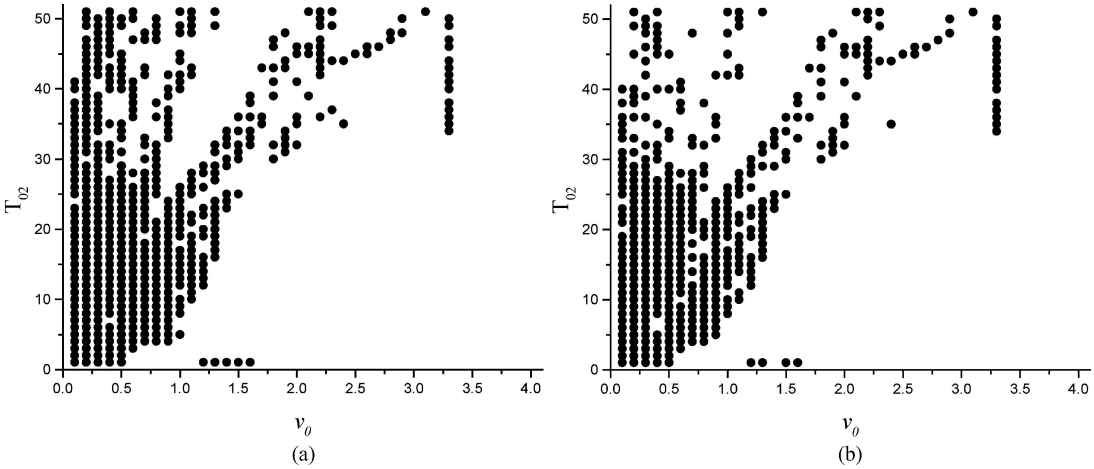

Figure 4. Domains of chaotic vibrations of the first (a) and of the second (b) oscillators in the (v_0, T_{02}) plane at $T_{01} = 29.43$.

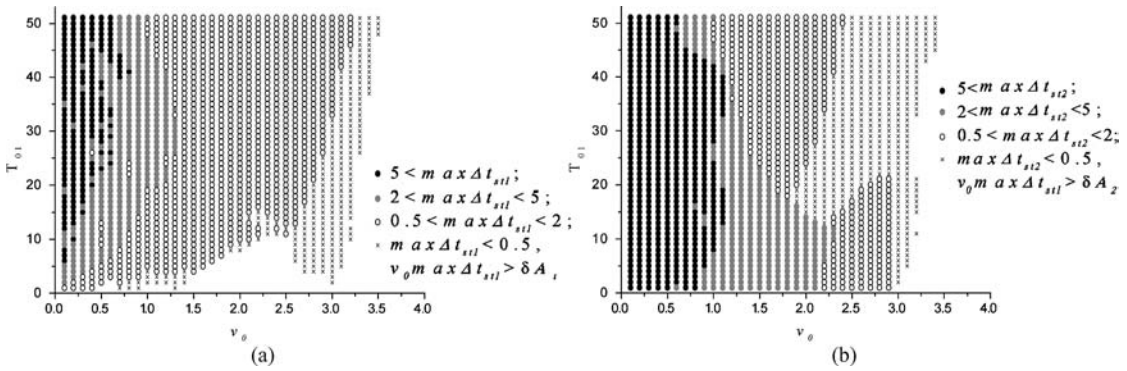

Figure 5. Domains of stick–slip oscillations of the first (a) and of the second (b) oscillators in the (v_0, T_{01}) plane at $T_{02} = 19.62$ for various stick conditions ($\delta = 0.1$).

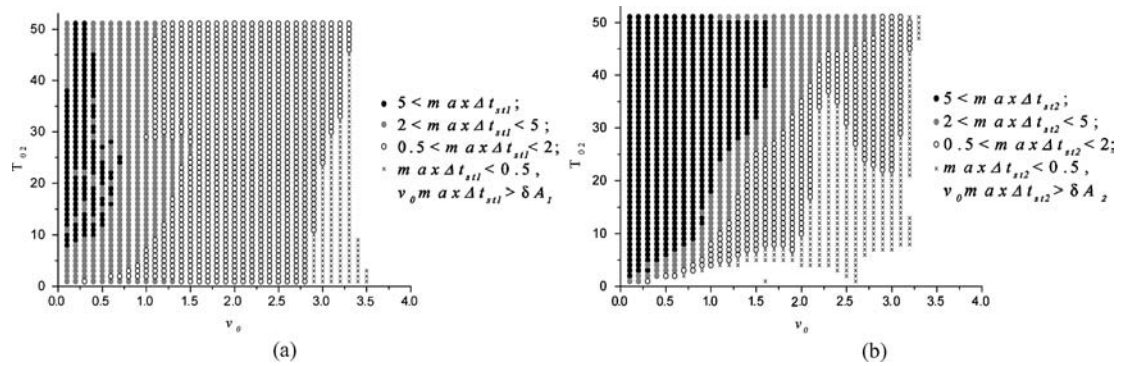

Figure 6. Domains of stick–slip oscillations of the first (a) and of the second (b) oscillators in the (v_0, T_{02}) plane at $T_{01} = 29.43$ for various stick conditions ($\delta = 0.1$).

$\Delta t_{\mathrm{st}\,i} < 2$). It is reported in the section $T_{02} = 19.62$ (see Figure 5) of the parameter space (v_0, T_{01}, T_{02}) for the first (a) and for the second (b) oscillators and also in the section $T_{01} = 29.43$ (see Figure 6) for the first (a) and for the second (b) oscillators. Crosses represent the domains in which max $\Delta t_{\mathrm{st}\,i} < 0.5$. But for these domains the stick segment on a phase plane, which corresponds to brief "adhesion" of an ith oscillator, exceeds δA_i. It is accepted $\delta = 0.1$. So, this segment exceeds a tenth of the characteristic vibrations amplitude of ith oscillator A_i. The latter behavior is caused by an increase in the dynamical process.

Now some examples characterizing the mentioned domains are presented.

Figure 7 shows the trajectories of the first and second oscillators on the phase plane for values of parameters $v_0 = 1$, $T_{01} = 30$, $T_{02} = 19.62$, which corresponds to the domain of the chaotic vibrations (see Figure 3(a) and (b)). Stick is corresponding to $2 <$ max $\Delta t_{\mathrm{st}\,i} < 5$ for the first oscillator and to $5 <$ max $\Delta t_{\mathrm{st}\,i}$ for the second oscillator (see Figure 5(a) and (b)). The phase portraits in Figure 8 are plotted for $v_0 = 0.9$, $T_{01} = 29.43$, $T_{02} = 15$. They correspond to chaotic domains, which are observed in Figure 4(a) and (b).

Figure 9 (for $v_0 = 2.5$, $T_{01} = 30$, $T_{02} = 19.62$) and Figure 10 (for $v_0 = 1.5$, $T_{01} = 0.5$, $T_{02} = 19.62$) represent periodic vibrations of both first and second oscillators. In Figure 10, the first oscillator moves without stick condition. All these data demonstrate a very good agreement with the obtained chaotic and regular vibration domains (see Figure 3) and with the domains of stick–slip and slip–slip motion (see Figure 5).

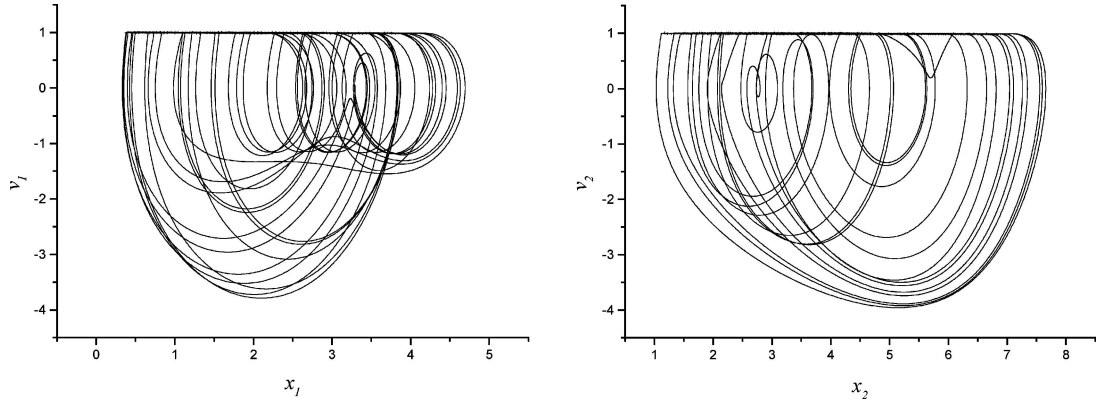

Figure 7. Phase portraits of the chaotic trajectories of the first and second oscillators ($v_0 = 1$, $T_{01} = 30$, $T_{02} = 19.62$) which correspond to the domains of the chaotic vibrations in the (v_0, T_{01}) plane. A stick refers to the maximum "adhesion" time of the oscillators to the belt: $2 < \max\Delta t_{st1} < 5$ for the first oscillator and $5 < \max\Delta t_{st2}$ for the second oscillator.

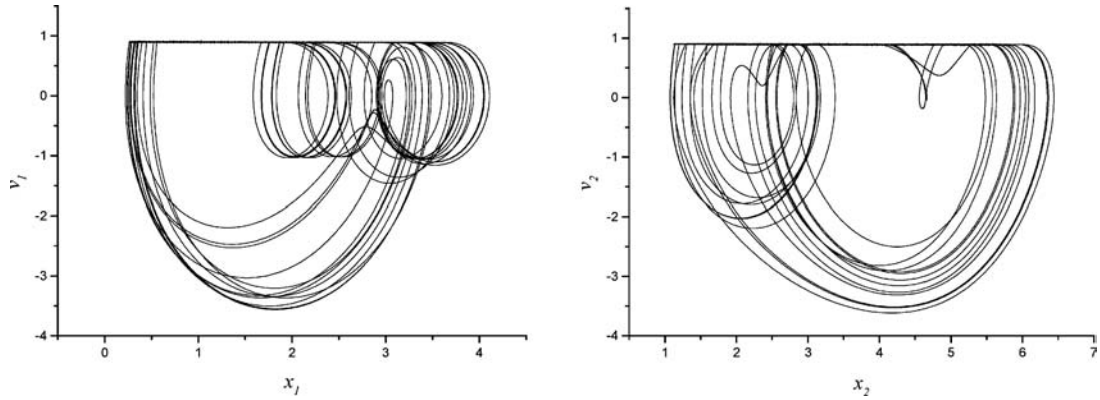

Figure 8. Phase portraits of the chaotic trajectories of the first and second oscillators ($v_0 = 0.9$, $T_{01} = 29.43$, $T_{02} = 15$) which correspond to the domains of the chaotic vibrations in the (v_0, T_{02}) plane. A stick refers to the maximum "adhesion" time of the oscillators to the belt: $2 < \max\ \Delta t_{st1} < 5$ for the first oscillator and $5 < \max\ \Delta t_{st2}$ for the second oscillator.

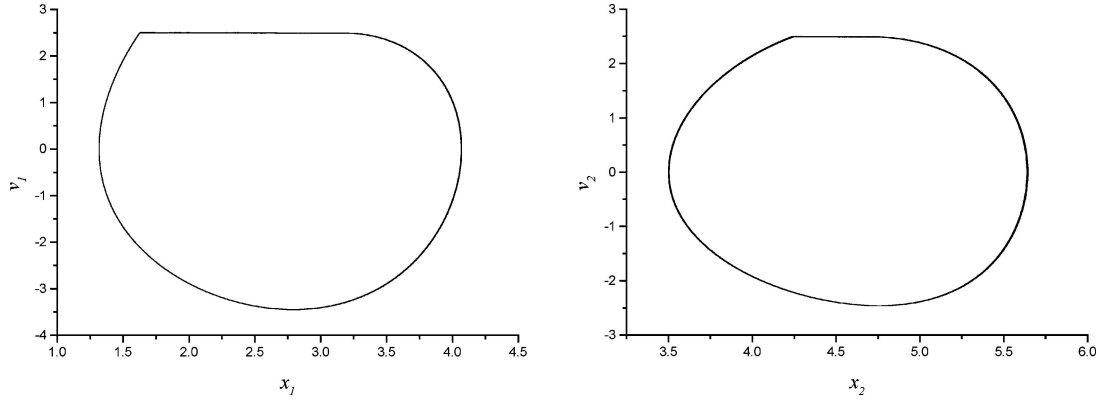

Figure 9. Phase portraits of the periodic trajectories of the first and second oscillators ($v_0 = 2.5$, $T_{01} = 30$, $T_{02} = 19.62$) which correspond to the domains of regular motion in the (v_0, T_{01}) plane. A stick refers to the maximum "adhesion" time of the oscillators to the belt: $0.5 < \max\ \Delta t_{st1} < 2$ for the first oscillator and $\Delta t_{st2} < 0.5$ for the second oscillator.

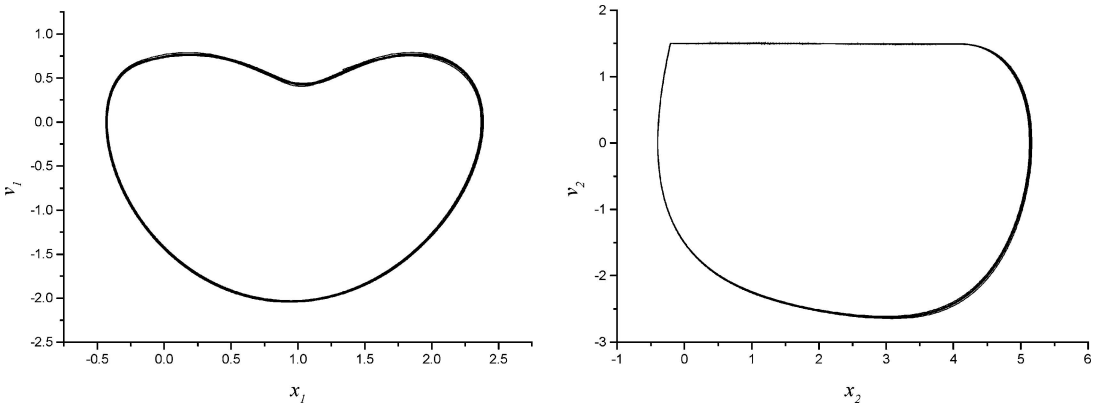

Figure 10. Phase portraits of the periodic trajectories of the first and second oscillators ($v_0 = 1.5$, $T_{01} = 0.5$, $T_{02} = 19.62$) which correspond to the domains of regular motion in the (v_0, T_{01}) plane. The first oscillator moves without a stick. A stick condition of the second oscillator refers to the maximum "adhesion" time to the belt $2 < \max \Delta t_{st2} < 5$.

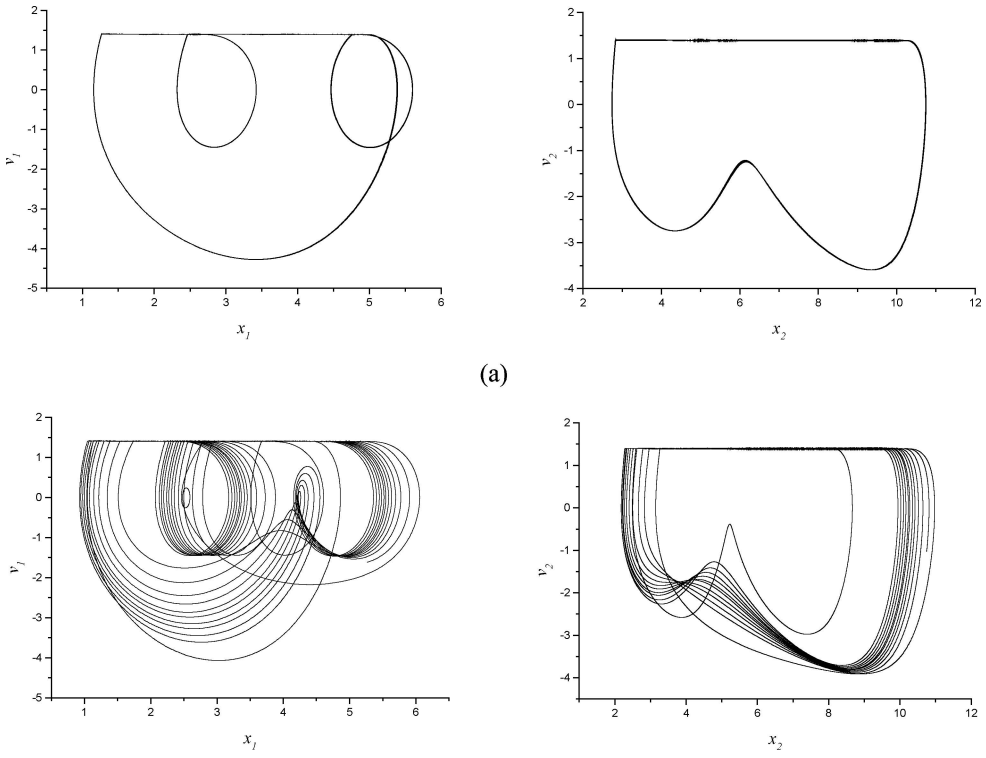

Figure 11. Phase portraits of the trajectories demonstrating "chaos onset" with a passage from the stability domain (a) ($v_0 = 1.4$, $T_{01} = 29.43$, $T_{02} = 40$) to the instability domain (b) ($v_0 = 1.4$, $T_{01} = 29.43$, $T_{02} = 34$).

In Figure 11, it is possible to observe "chaos onset" with a passage from the stability domain (a) at fixed values of parameters $v_0 = 1.4$, $T_{01} = 29.43$, $T_{02} = 40$ to the instability domain (b) at fixed values of parameters $v_0 = 1.4$, $T_{01} = 29.43$, $T_{02} = 34$ (see also Figure 4). In the first case, one can see the regular motion about the three states. Then the first oscillator wanders around these states with unpredictable jumping.

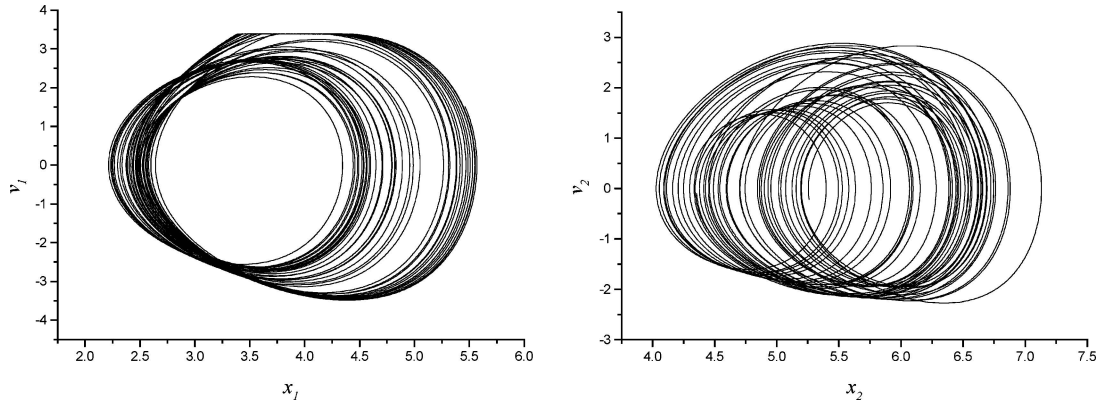

Figure 12. Phase portraits of the trajectories of the first and second oscillators ($v_0 = 3.4$, $T_{01} = 41$, $T_{02} = 19.62$). The second oscillator is in a slip–slip chaotic motion.

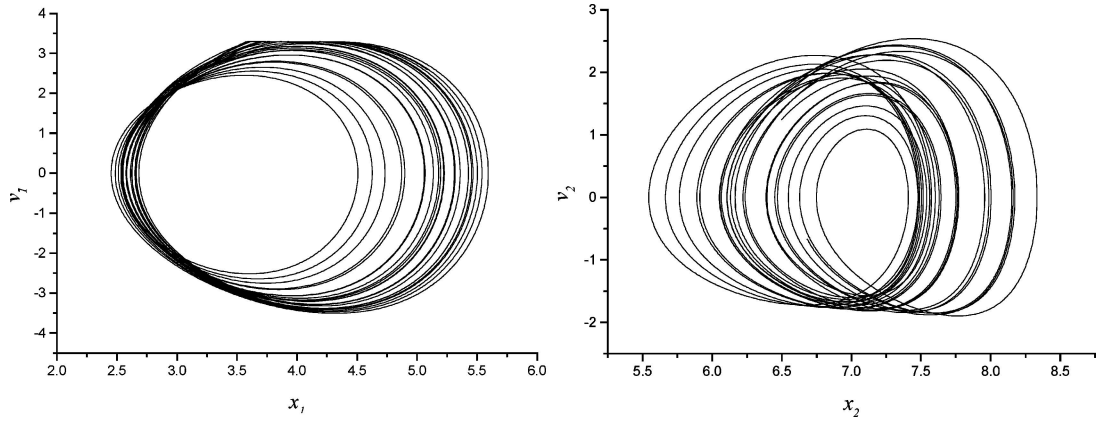

Figure 13. Phase portraits of the trajectories of the first and second oscillators ($v_0 = 3.3$, $T_{01} = 29.43$, $T_{02} = 36$). The second oscillator is in a slip–slip chaotic motion.

The comparison between Figure 3 and Figure 5, and also between Figure 4 and Figure 6 yield a conclusion that mainly stick–slip chaos is observed during our experiments. Slip–slip chaotic motion is exhibited only in the small domain in a neighborhood of $v_0 = 3.3$–3.4, and only for the second oscillator. Examples are shown in both Figure 12 for fixed values of parameters $v_0 = 3.4$, $T_{01} = 41$, $T_{02} = 19.62$ and Figure 13 for fixed values of parameters $v_0 = 3.3$, $T_{01} = 29.43$, $T_{02} = 36$.

6. Conclusions

Our approach designed to quantify regular and chaotic domains were successfully applied to analyze stick–slip and slip–slip dynamics in our self-excited 2-degrees-of-freedom system with friction. Both stick–slip and slip–slip periodic and chaotic trajectories are studied. It is shown, among others, that for a wide interval of investigated parameters a stick–slip dynamics dominates. Our investigations show that the situation when only one of the oscillators moves chaotically is not observed. However, there are conditions when only the first oscillator moves with "adhesion" to the belt and the other oscillator moves without "adhesion", and vice versa.

In addition, our numerical tests indicate that our direct technique is less time consuming that the standard approaches devoted for the computation of Lyapunov exponents when considering discontinuous systems [13].

Acknowledgements

This work has been partially supported by the Polish State Committee for Scientific Research (Grant No. 5 T07A 019 23). CG was supported by FAPESP and CNPq.

References

1. Awrejcewicz, J., *Bifurcation and Chaos in Simple Dynamical Systems*, World Scientific, Singapore, 1989.
2. Awrejcewicz, J., *Bifurcation and Chaos in Coupled Oscillators*, World Scientific, Singapore, 1991.
3. Woafo, P., Chedjou, J. C., and Fotsin, H. B., 'Dynamics of a system consisting a Van der Pol oscillator coupled to a Duffing oscillator', *Physics Reviews E* **54**, 1996, 5929–5934.
4. Awrejcewicz, J. and Delfs, J., 'Dynamics of a self-exicted stick–slip oscillator with two degrees of freedom. Part I: Investigation of equilibria', *European Journal of Mechanics, A/Solids* **9**(4), 1990, 269–282.
5. Awrejcewicz, J. and Delfs, J., 'Dynamics of a self-exicted stick–slip oscillator with two degrees of freedom. Part II: Slip–stick, slip–slip, stick–slip transitions, periodic and chaotic orbits', *European Journal of Mechanics, A/Solids* **9**(5), 1990, 397–418.
6. Awrejcewicz, J. and Holicke, M. M., 'Melnikov's method and stick–slip chaotic oscillations in very weekly forced mechanical systems', *International Journal of Bifurcation and Chaos* **9**(3), 1999, 505–518.
7. Chedjou, J. C., Woafo, P., and Domnganag, S., 'Shilnikov chaos and dynamics of a self-sustained electromechanical transducer', *Journal of Sound and Vibration* **123**, 2001, 170–174.
8. Awrejcewicz, J. and Calvisi, M. L., 'Mechanical models of Chua's circuit', *International Journal of Bifurcation and Chaos* (Tutorial Paper) **12**(4), 2002, 671–686.
9. Savi, M. A. and Pacheco, P. M. L. C., 'Chaos and hyperchaos shape memory systems', *International Journal of Bifurcation and Chaos* **12**(3), 2002, 645–657.
10. Steigenberger, I., *Statics of an artificial worm segment*, TU Ilmenau, Fac. Math. Nat. Sci., Preprint No M04/01.
11. Kunze, M., 'Non-smooth dynamical systems', in *Lecture Notes in Mathematics*, Vol. 1744, Springer-Verlag, Berlin, 2000.
12. Dzyubak, L., 'Investigation of chaos appearance in the nonlinear dynamical systems based on analysis of the wandering trajectories', in *Proceedings of the 6th Conference on Dynamical Systems – Theory and Applications*, Lodz, Poland, December 10–12, 2001, pp. 243–248.
13. Muller, P. C., 'Calculation of Lyapunov exponents for dynamic systems with discontinuities', *Chaos, Solitons and Fractals* **5**(9), 1995, 1671–1681.
14. Hsu, C. S., 'A theory of cell-to-cell mapping dynamical systems', *ASME Journal of Applied Mechanics* **47**, 1980, 931–939.
15. Hsu, C. S., 'A generalized theory of cell-to-cell mapping for nonlinear dynamical systems', *ASME Journal of Applied Mechanics* **48**, 1981, 634–642.
16. Hsu, C. S., Guttalu, R. S., and Zhu, W. H., 'A method of analyzing generalized cell mappings', *ASME Journal of Applied Mechanics* **49**, 1982, 885–894.
17. Gruendler, J., 'The existence of homoclinic orbits and the method of Melnikov for systems in Rn', *SIAM Journal of Mathematical Analysis* **16**(5), 1985, 907–931.
18. Sprott, J. C., *Chaos and Time-Series Analysis*, Oxford University Press, New York, 2003.